Excavating an Active Site: The Nucleobase Specificity of Ribonuclease A†

Bradley R. Kelemen,[‡,§] L. Wayne Schultz,[‡,||] Rozamond Y. Sweeney,[‡] and Ronald T. Raines*[,‡,⊥]

Department of Biochemistry and Department of Chemistry, University of Wisconsin—Madison, Madison, Wisconsin 53706

Received August 8, 2000; Revised Manuscript Received September 28, 2000

ABSTRACT: Ribonuclease A (RNase A) catalyzes the cleavage of RNA after pyrimidine nucleotides. When bound in the active site, the base of a pyrimidine nucleotide forms hydrogen bonds with the side chain of Thr45. Here, the role of Thr45 was probed by using the wild-type enzyme, its T45G variant, X-ray diffraction analysis, and synthetic oligonucleotides as ligands and substrates. Catalytic specificity was determined with the fluorogenic substrate: 6-carboxyfluorescein∼dArXdAdA∼6-carboxytetramethylrhodamine (6-FAM∼dArXdAdA∼6-TAMRA), where X = C, U, A, or G. Wild-type RNase A cleaves 10^6-fold faster when X = C than when X = A. Likewise, its affinity for the non-hydrolyzable oligonucleotide 6-FAM∼d(CAA) is 50-fold greater than for 6-FAM∼d(AAA). T45G RNase A cleaves 6-FAM∼dArAdAdA∼6-TAMRA 10^2-fold faster than does the wild-type enzyme. The structure of crystalline T45G RNase A, determined at 1.8-Å resolution by X-ray diffraction analysis, does not reveal new potential interactions with a nucleobase. Indeed, the two enzymes have a similar affinity for 6-FAM∼d(AAA). The importance of pentofuranosyl ring conformation to nucleotide specificity was probed with 6-FAM∼d(AU^FAA), where U^F is 2′-deoxy-2′-fluorouridine. The conformation of the pentofuranosyl ring in dU^F is known to be more similar to that in rU than dU. The affinity of wild-type RNase A for 6-FAM∼d(AU^FAA) is 50-fold lower than for 6-FAM∼d(AUAA). This discrimination is lost in the T45G enzyme. Together, these data indicate that the side chain of Thr45 plays multiple roles—interacting favorably with pyrimidine nucleobases but unfavorably with purine nucleobases. Moreover, a ribose-like ring disfavors the interaction of Thr45 with a pyrimidine nucleobase, suggesting that Thr45 enhances catalysis by ground-state destabilization.

Life relies on the specificity of biomolecular recognition. Of foremost importance is the specificity with which enzymes recognize their substrates and nucleic acid-binding proteins recognize their cognate nucleic acids. Here, we illuminate the pivotal role of one amino acid residue in the recognition of RNA by an enzyme, bovine pancreatic ribonuclease A [RNase A[1] (*1, 2*); EC 3.1.27.5].

RNase A catalyzes the cleavage of single-stranded RNA. Over 50 years ago, this cleavage was demonstrated to occur preferentially on the 3′ side of pyrimidine nucleotides (*3*−*5*). Over 30 years ago, the "amide" portion of the pyrimidine nucleobase (that is, $-C^2(O)-N^3=$ in cytosine and $-C^2(O)-N^3(H)-$ in uracil) was shown to be critical for recognition by the enzyme (*6*). The determination of the structure of crystalline RNase A (*7*) lead to the proposal that the specificity of RNase A was enforced by the interaction of the pyrimidine nucleobase with a particular active-site residue: Thr45 (*8*). This threonine residue, which is conserved in all of the >40 known members of the RNase A superfamily (*9*), forms hydrogen bonds with a cytosine or uracil base of a bound nucleic acid (Figure 1) (*10, 11*). Recently, site-directed mutagenesis has revealed that these hydrogen bonds effect the cytosine versus uracil nucleobase specificity of RNase A (*12, 13*) as well as its homolog, human angiogenin (*14*). The catalytic specificity of RNase A for poly(cytidylic acid) [poly(C)] over poly(adenylic acid) [poly(A)] is profound, with a relative k_{cat}/K_m value of 10^4 (*13*). RNase A does not appear to catalyze the cleavage of poly(guanylic acid) [poly(G)].

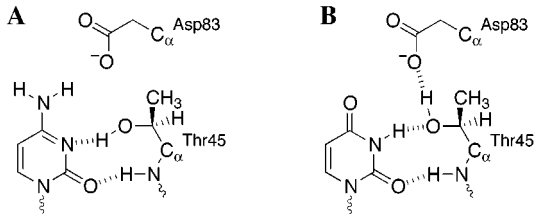

FIGURE 1: Hydrogen bonds formed between the residues of the B1 subsite of ribonuclease A and a bound cytidine nucleotide (*11*) (A) and a bound uridine nucleotide (*10*) (B).

How does Thr45 mediate nucleobase recognition by RNase A? To answer this question, we excavate the active

† This work was supported by Grant GM44783 (NIH). B.R.K. was supported by Chemistry-Biology Interface Training Grant GM08506 (NIH). R.Y.S was a Mary Shine Peterson undergraduate scholar. L.W.S. was supported by Postdoctoral Fellowship CA69750 (NIH).

* To whom correspondence should be addressed. Telephone: (608)-262-8588. Fax: (608)262-3453. E-mail: Raines@biochem.wisc.edu.

‡ Department of Biochemistry.

§ Present address: Promega Corp., 2800 Woods Hollow Rd., Madison, WI 53711-5399.

|| Present address: Hauptman-Woodward Medical Research Institute, 73 High St., Buffalo, NY 14203-1196.

⊥ Department of Chemistry.

[1] Abbreviations: dG^F, 2′-deoxy-2′-fluoroguanidine; dU^F, 2′-deoxy-2′-fluorouridine; 6-FAM, 6-carboxyfluorescein; 6-TAMRA, 6-carboxytetramethylaminorhodamine; PDB, Protein Data Bank (http://www.rcsb.org/pdb/); poly(A), poly(adenylic acid); poly(C), poly(cytidylic acid); rms, root mean square; RNase A, bovine pancreatic ribonuclease A.

10.1021/bi001862f CCC: $19.00
Published on Web 11/02/2000

site—eliminating the side chain of Thr45 by creating the T45G variant. We determine the structure of crystalline T45G RNase A at high resolution and compare this structure to that of the wild-type enzyme. We use fluorescence anisotropy to determine the binding affinity of synthetic substrate analogues to wild-type RNase A and the T45G variant, and we use analogous synthetic fluorogenic substrates to probe substrate turnover by the two enzymes. We find that Thr45, which does not participate directly in the cleavage or formation of covalent bonds, plays a multitude of roles in the binding and turnover of substrates by RNase A.

EXPERIMENTAL PROCEDURES

Materials. All materials were of commercial reagent grade or better and were obtained as we described previously (*15*, *16*).

Protein Production and Purification. Replacing Thr45 with a glycine residue enabled us to reveal the contribution of the entire side chain of Thr45 to nucleobase specificity. T45G RNase A was produced and purified by methods described previously (*12*, *13*). Briefly, T45G RNase A was produced in inclusion bodies in *Escherichia coli* cells. These cells were lysed by passage through a French pressure cell. Inclusion bodies were isolated by centrifugation and then reduced and denatured. T45G RNase A was oxidatively folded and purified by gel filtration chromatography followed by cation-exchange chromatography. The protein solution was then dialyzed exhaustively against water and lyophilized. Wild-type RNase A was produced by a similar method and was a generous gift of B. M. Fisher. T45G RNase A has a T_m (which is the temperature at the midpoint of the thermal transition) of 53 °C (*13*), which is 10 °C lower than that of the wild-type enzyme but still 28 °C higher than the temperature at which assays were performed herein.

Analytical Instrumentation. Time-based fluorescence readings were collected with excitation at 490 nm and emission at 515 nm using a QuantaMaster QM1 fluorometer from Photon Technologies International (South Brunswick, NJ) equipped with stirring and temperature control. Fluorescence anisotropy was measured at room temperature (23 ± 2 °C) on a Beacon fluorescence polarization system from PanVera (Madison, WI). Wild-type and T45G RNase A concentration was determined by using $\epsilon = 0.72$ mL mg^{-1} cm^{-1} at 277.5 nm in a Cary model 50 spectrophotometer from Varian (Sugar Land, TX) equipped with a temperature controller.

Structure of Crystalline T45G Ribonuclease A. Protein Crystallization. Crystals of T45G RNase A were prepared by vapor diffusion using the hanging drop method. Drops (6 μL) of 0.050 M sodium acetate buffer (pH 5.6) containing T45G RNase A (60 mg/mL), ammonium sulfate (15% w/v), and sodium chloride (25% w/v) were suspended over wells (1.0 mL) of 0.10 M sodium acetate buffer (pH 5.6) containing ammonium sulfate (30% w/v) and sodium chloride (50% w/v). Single tetragonal crystals grew out of amorphous precipitate at 20 °C, appeared within 3 days, and grew to a final size of 0.7 × 0.7 × 0.7 mm.

Data Collection. The crystals of T45G RNase A were of space group $P3_221$, with $a = 64.32$ Å, $c = 64.84$ Å, $\alpha = \beta = 90°$, and $\gamma = 120°$. X-ray data were collected with a Siemens HI-STAR detector mounted on a Rigaku rotating anode operating at 50 kV, 90 mA, and a 300-μm focal spot.

Table 1: X-ray Diffraction Analysis Statistics for T45G Ribonuclease A

space group	$P3_221$
cell dimensions (Å)	$a = 64.32$ (1) $b = 64.32$ (1) $c = 64.84$ (2) $\alpha = \beta = 90°$ $\gamma = 120°$
protein molecules/unit cell	6
Data Collection Statistics	
resolution (Å)	1.8
no. of measured refections ($I/\sigma > 0.33$)	62164
no. of unique reflections	18761
average redundancy	3.3
average I/σ	23.2
completeness of data (30−1.8 Å)	96%
completeness of high-resolution shell (1.9−1.8 Å)	87%
R_{sym} ($I/\sigma > 0.33$)[a]	0.036
R_{sym} (1.9−1.8 Å)[a]	0.19
Final Refinement Statistics	
RNase A atoms	968
solvent atoms	120
R-factor (30.0−1.8 Å) [b]	0.176
rms deviations from ideal geometry	
bond distances (Å)	0.011
bond angles (deg)	2.4
average *B*-factors (Å^2)	
protein (main chain)	25.1
protein side chain and solvent	35.7
acetate	38.5
chloride	11

[a] $R_{sym} = \Sigma_{hkl}|I - \langle I\rangle|\Sigma_{hkl}I$, where I is the observed intensity and $\langle I\rangle$ is the averaged intensity obtained from multiple observations of symmetry related reflections. [b] *R*-factor $= \Sigma_{hkl}|F_o - F_c|/\Sigma_{hkl}|F_o|$, where F_o and F_c are the observed and calculated structure factors, respectively.

The X-ray beam was collimated by double-focusing mirrors. The crystal-to-detector distance was 12.0 cm. Data were obtained in 512 × 512 pixel format, processed with the program XDS (*17*, *18*) and scaled with the program XSCALIBRE (G. Wesenberg and I. Rayment, unpublished results). Frames of data were collected from a single crystal using ϕ-scans. Reflections with $I/\sigma < 0.33$ were rejected. The crystal was cooled in a 4 °C air stream, resulting in negligible crystal decay for the entire data collection. Full crystallographic details are listed in Table 1.

Refinement. Prior to least-squares refinement $2|F_o| - |F_c|$, $|F_o| - |F_c|$, and σA (*19*) difference maps were calculated using the data from 30 to 3.5 Å. The model was examined and was continuous in the density for the entire chain. Nonetheless, there was some disorder apparent in the C-terminus, from His119 to Ala122. The starting model (PDB entry 7RSA minus residues 119−122) was subjected to 10 cycles of least-squares refinement with the program TNT (*20*) and the data from 30 to 3.0 Å, giving an initial *R*-factor of 0.252. A negative difference Fourier map ($|F_o| - |F_c|$) showed clearly the absence of the Thr45 side chain. The Thr45 side chain was removed, and the model was refined to 2.0 Å. Manual adjustments to the model were performed with the program TURBO−FRODO (*21*). The model was further refined to 1.8 Å, and the difference map ($|F_o| - |F_c|$) showed two clear conformations for residues 119−122. These residues were fitted and refined in two separate conformations with 50% occupancy for each (determined iteratively). After several cycles of manual adjustments and least-squares refinement, water molecules were added to the model. The peak-searching algorithm in

TNT was used to place ordered water molecules. Water molecules were retained if they had at least 1σ of $2|F_o| - |F_c|$ density and 3σ of $|F_o| - |F_c|$ density and were within hydrogen bonding distance of the protein or other water molecules.

Design of Oligonucleotide Ligands and Substrates. Thr45 is the major component of the enzymic B1 subsite, which has a strong preference for pyrimidine nucleobases. RNase A has two other known nucleobase-binding subsites. The B2 subsite has a preference for an adenine base, and the B3 subsite has a preference for a purine base.[2] Thus, the preferred substrate for RNase A is YAR, where Y refers to a pyrimidine nucleotide and R refers to a purine nucleotide (*23*).

We took advantage of the specificity of B2 and B3 subsites in designing oligonucleotide ligands and substrates for this study. Our synthetic oligonucleotides all contain the trinucleotide: XAA, with X being variable. RNase A has a strong tendency to bind XAA with the nucleobase of X residing in the B1 subsite. For example, the structure of the crystalline complex of RNase A with d(ATAAG) shows that T, A, and A occupy the B1, B2, and B3 subsites, respectively (*22*).[2]

Equilibrium Dissociation Constants. Values of the equilibrium dissociation constants (K_d) for the complexes of wild-type RNase A and the T45G variant with oligonucleotide ligands were determined with fluorescence anisotropy (*24*−*26*). Oligonucleotide ligands were from Promega (Madison, WI), and were produced from commercially available reagents and purified by extraction from a polyacrylamide gel after electrophoresis. The ligands were of the form 6-FAM∼d(UAA), 6-FAM∼d(CAA), 6-FAM∼d(AAA), 6-FAM∼d(ØAA), 6-FAM∼d(AUAA), and Fl-(dAU^{F}AA), where Ø refers to a residue in which a nucleobase is replaced with a hydrogen atom, U^F refers to 2′-deoxy-2′-fluorouridine, and 6-FAM refers to 6-carboxyfluorescein attached to the 5′ end of the oligonucleotides by a six-carbon spacer through a terminal 5′ phosphoryl group (Figure 2). The concentration of 6-FAM∼d(AUAA) and 6-FAM∼d(AU^{F}AA) was determined by using $\epsilon = 66\,300$ M^{-1} cm^{-1} at 260 nm. The concentration of 6-FAM∼d(UAA), 6-FAM∼d(CAA), 6-FAM∼d(AAA), and 6-FAM∼d(ØAA) was determined by using $\epsilon = 51\,100$, 49 700, 57 900, and 42 700 M^{-1} cm^{-1} at 260 nm, respectively (*27*).

Wild-type RNase A or the T45G variant (1−2 mM) was dissolved in 2.00 mL of 0.020 M MES−NaOH buffer (pH 6.0) containing NaCl (0.050 M) for the tetranucleotide ligands or in 2.00 mL of 0.10 M MES−NaOH buffer (pH 6.0) containing NaCl (0.10 M) for the trinucleotide ligands. The protein sample was filtered and partitioned between a sample tube (0.90 mL) and a blank tube (0.90 mL). Oligonucleotide ligand (0.10 mL of a 0.10 μM solution in the appropriate buffer) was added to the sample tube, and buffer (0.10 mL) was added to the blank tube. The anisotropy of each sample was measured 3−5 times with the blank reading taken before each sample. The anisotropy values were averaged. The sample was diluted by removing an aliquot (0.25 mL), which was replaced with an equal volume of ligand (10 nM) in buffer. The blank was diluted similarly, with an equal volume of buffer added. The anisotropy of each sample was again measured 3−5 times, with the blank read before each sample and the anisotropy values averaged. This process was repeated up to 20 times to complete each binding isotherm. At the end of the experiment, the exact protein concentrations of both the blank and the sample for the first five protein concentrations were determined by their absorbance at 277.5 nm. The remaining protein concentrations were calculated from the dilutions at each step.

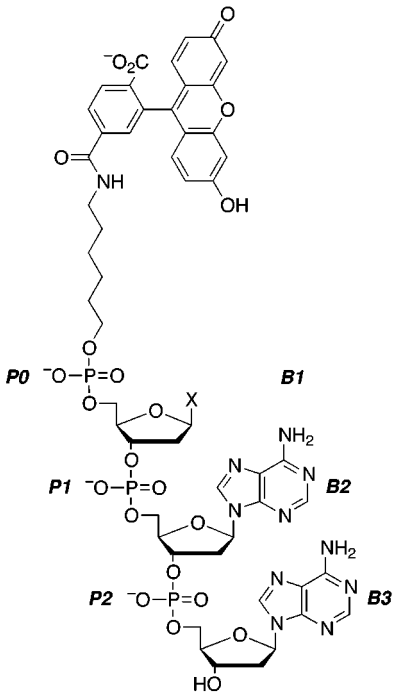

FIGURE 2: Deoxynucleotides labeled with 6-carboxyfluorescein used to assess binding to the B1 subsite of ribonuclease A. The italicized text refers to enzymic subsites known to interact with nucleobases (B1, B2, and B3) and phosphoryl groups (P0, P1, and P2) (*49*). X = Ade, Cyt, Ura, or H (abasic).

Values of K_d were determined by weighted, nonlinear least-squares fitting of the data to eq 1 with the program DELTAGRAPH4.0 from DeltaPoint (Monterey, CA):

$$A = \frac{\Delta A[\text{RNase A}]}{K_d + [\text{RNase A}]} + A_{min} \qquad (1)$$

In eq 1, A is the average of the measured anisotropy values, ΔA ($= A_{max} - A_{min}$) is the difference in anisotropy values of bound and free ligand, A_{min} is the anisotropy of the unbound ligand, [RNase A] is the total protein concentration (which is assumed to equal the concentration of unliganded protein), and K_d is the equilibrium dissociation constant.

Steady-State Kinetic Analyses. Values of k_{cat}/K_m for the cleavage of oligonucleotide substrates by wild-type RNase A and the T45G variant were determined with fluorescence spectroscopy. Oligonucleotide substrates were a generous gift from Integrated DNA Technologies (Coralville, IA), and were synthesized from commercial reagents as we described previously (*15*). These substrates were of the form 6-carboxyfluorescein∼dArXdAdA∼6-carboxytetramethylrhodamine (6-FAM∼dArXdAdA∼6-TAMRA), where X is

[2] The existence of the B3 subsite has been inferred from kinetic data and chemical modification studies (*2*). In the crystalline RNase A·d(ATAAG) complex, the adenine base in the B3 subsite stacks with the adenine base in the B2 subsite (*22*). The B3 "subsite" could therefore result from $\pi-\pi$ stacking interactions that stabilize the enzyme·nucleic acids complex solely by preorganization or desolvation of the nucleic acid.

uridine, cytidine, adenosine, or guanine. Assays with these fluorogenic substrates are based on the quenching of fluorescence of 6-FAM held in proximity to 6-TAMRA by a single ribonucleotide embedded within three deoxyadenosine nucleotides (*15*). When RNase A cleaves the sole ribosyl unit, the fluorescein moiety is released from its proximity to the rhodamine moiety and manifests its intrinsic fluorescence. The concentrations of 6-FAM∼dArCdAdA∼6-TAMRA,6-FAM∼dArUdAdA∼6-TAMRA,6-FAM∼dArAdAdA∼6-TAMRA, or 6-FAM∼dArGdAdA∼6-TAMRA were determined by using ϵ = 99 900, 102 000, 108 000, and 104 000 M^{-1} cm^{-1} at 260 nm, respectively (*27*).

Assays were carried out in a 2.00-mL volume of 0.10 M MES−NaOH buffer (pH 6.0) containing NaCl (0.10 M), substrate (5.0−20 nM), and wild-type RNase A (1.0 pM−1.0 μM), or T45G RNase A (5.0 nM−0.30 μM). Data collected in this manner were fitted to eqs 2 or 3, depending on the extent of product formation during the course of data collection (*15*), with the program DELTAGRAPH4.0:

$$I = I_f - (I_f - I_o)e^{-kt} \quad (2)$$

$$I = I_o + (I_f - I_o)k_{obs}t \quad (3)$$

The intensity of fluorescence (I) was recorded in units of photon counts/s. Product fluorescence intensity (I_f) was determined for each experiment by nonlinear least-squares regression analysis using eq 3 after the addition of sufficient enzyme to complete the reaction within 30 min. T45G RNase A was used to determine product intensity for 6-FAM∼dArAdAdA∼6-TAMRA, and ribonuclease T1 from Sigma Chemical (St. Louis, MO) was used to determine product intensity for 6-FAM∼dArGdAdA∼6-TAMRA. Substrate fluorescence intensity (I_o) was determined by averaging data collected for 2−5 min prior to enzyme addition. The pseudo-first-order rate constants, k and k_{obs}, were determined at substrate concentrations below K_m (*15*). Values of k_{cat}/K_m were determined by dividing the psuedo-first-order rate constant by the enzyme concentration. Values of k_{cat}/K_m determined in this manner were independent of enzyme and substrate concentration within the experimental range of substrate and enzyme concentrations (data not shown).

RESULTS

Crystalline Structure of T45G Ribonuclease A. The structure of T45G RNase A was refined to an *R*-factor of 0.176 using data from 30 to 1.8 Å (Table 1). The root mean square (rms) deviation from ideal bond lengths is 0.011 Å, and the rms deviation from ideal bond angles is 2.4°. The average *B*-factors are 25.1 $Å^2$ for main-chain atoms and 38.7 $Å^2$ for side-chain atoms. The electron density is continuous for the main chain and most side chains. The presence of Gly45 (or absence of Thr45) is unambiguous and clearly defined in both $2|F_o| - |F_c|$ density and annealed omit $|F_o| - |F_c|$ density. Atomic coordinates for T45G RNase A were deposited in the Protein Data Bank (PDB) with accession code 3RST.

The overall structure of T45G RNase A shows little variation from that of wild-type RNase A (main-chain rms deviation of 0.61 Å from PDB entry 7rsa) with the largest deviation occurring in the main chain of residues Lys66 and Asn67 (Figure 3A). The side-chain residues proximal to Gly45 are less resolved than those same residues in wild-type RNase A (Figure 3B). The side chain of Ile81 is directly adjacent to Gly45 and occupies two conformations (χ_{1A} = 64° and χ_{1B} = 173°). The side chain of Asp83 also occupies two conformations (χ_{1A} = −72° and χ_{1B} = −165°). Similarly, Asp83 of wild-type RNase A (PDB entry 7RSA) exists in two conformations (χ_{1A} = −110° and χ_{1B} = −179°), which differ from those in the structure of T45G RNase A.

The side chain of Phe120, part of the enzymic B1 subsite (*23*), has density for all but the $C_{\epsilon 1}$, $C_{\epsilon 2}$, and C_ζ atoms and occupies a different conformation (χ_1 = −115° and χ_2 = 160°) than that observed in the wild-type RNase A crystalline structure (χ_1 = −169° and χ_2 = −85°). The main-chain carbonyl of Phe120 exists in two positions (ϕ_A = −90° and ψ_A = 149°; ϕ_B = −100° and ψ_B = 100°). This dichotomy has not been observed for Phe120 of wild-type RNase A (ϕ = −98° and ψ = 116°).

As in some crystalline structures of wild-type RNase A, the active-site residue His119 in the T45G variant occupies two positions, referred to as A and B (χ_{1A} = 175° and χ_{1B} = −59°). The electron density defining the A position is not, however, substantial enough to establish exact rotation about the χ_2 angle of this residue. For this reason, we caution against over-interpretation of distances to His119 in the A position. In the A position of the T45G RNase A crystalline structure, His119 is within hydrogen-bonding distance from one of two conformations of the main-chain carbonyl of Phe120 (distance of 2.5 Å from $N_{\epsilon 2}$ of His119 to NH of Phe120). In the wild-type structure, the side chain of His119 forms a hydrogen bond with Asp121 (distance of 2.91 Å from $N_{\epsilon 2}$ of His119 to $O_{\delta 1}$ of Asp121). This hydrogen bond is not present in the structure of T45G RNase A (distance of 4.35 Å from $N_{\epsilon 2}$ of His119 to $O_{\delta 1}$ of Asp121).

The main-chain carbonyl of residue 45 forms a hydrogen bond with $N_{\delta 1}$ of His12, as is observed in the wild-type structure. Likewise, the side chain of Asp121 forms a hydrogen bond with the main chain of Lys66, as in the wild-type structure. A conserved water molecule is also present in a hydrogen-bonding network despite the movement of residues Lys66 and Asn67 away from the active site. These residues are displaced by an rms deviation of 1.5 Å from their position in wild-type RNase A.

An acetate molecule is present in the active site and interacts with His12 (distance of 2.65 Å from $N_{\epsilon 2}$ to O_2 of acetate), the main chain of Phe120 (distance of 3.22 Å from NH to O_1 of acetate), and His119 (distance of 2.59 Å from $N_{\delta 1}$ to O_1 of acetate). There also exist three chloride ions in the structure in positions similar to those observed by Almo and co-workers (*28*).

Binding Specificity of Ribonuclease A. The values of K_d for the complex of wild-type RNase A and the T45G variant with four deoxynucleotides, 6-FAM∼d(CAA), 6-FAM∼d(UAA), 6-FAM∼d(AAA), and 6-FAM∼d(ØAA), were determined by fluorescence anisotropy (Figure 4A). These values are listed in Table 2 and depicted in Figure 4B. Wild-type RNase A has more affinity for pyrimidine nucleotides, 6-FAM∼d(CAA) and 6-FAM∼d(UAA), than for nucleotides that contain either adenosine or an abasic analogue of DNA, 6-FAM∼d(AAA) and 6-FAM∼d(ØAA). In contrast, T45G RNase A has an approximately equal affinity for 6-FAM∼d(CAA), 6-FAM∼d(UAA), 6-FAM∼d(AAA), and 6-FAM∼d(ØAA).

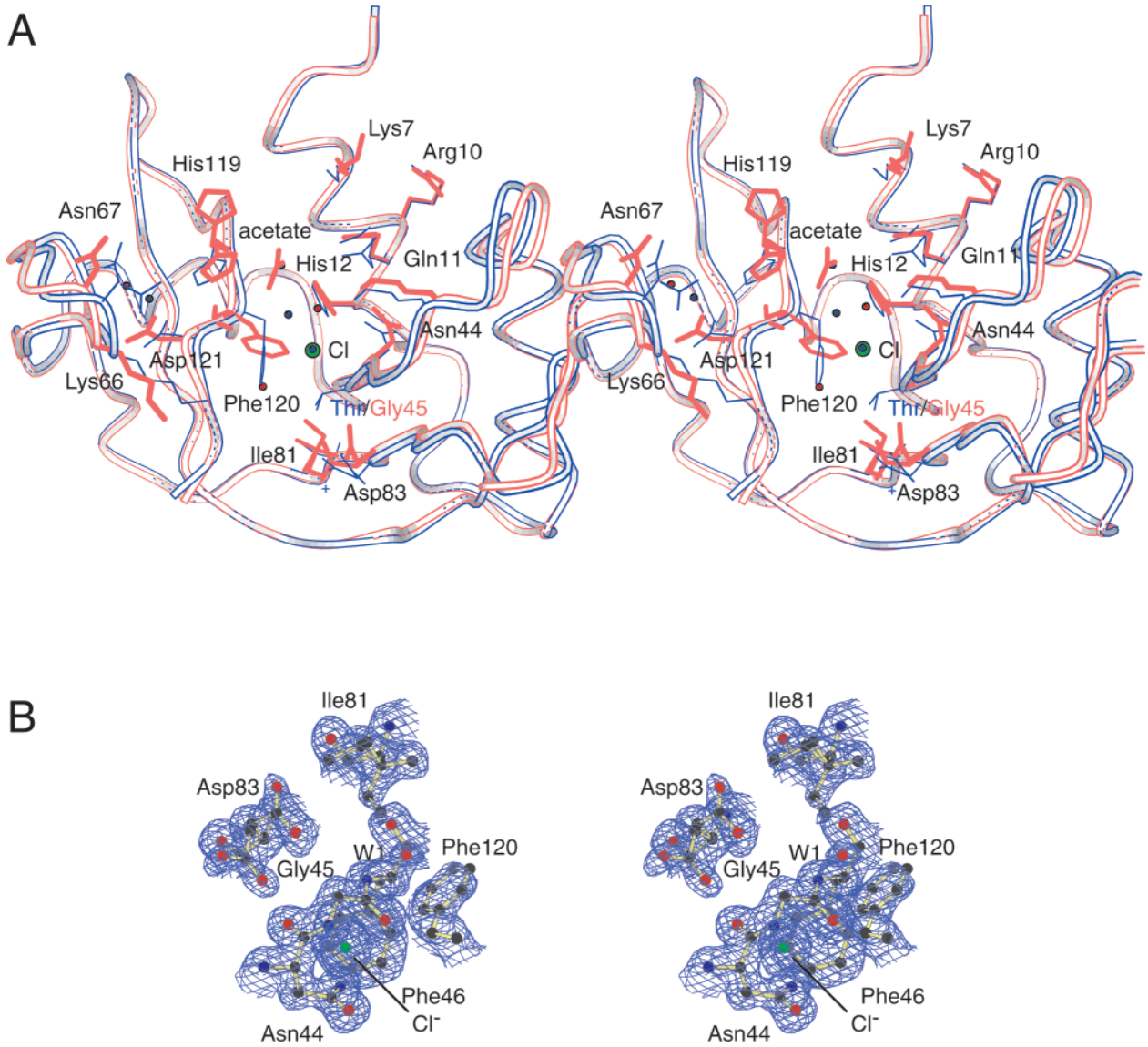

FIGURE 3: Three-dimensional structure of T45G ribonuclease A. (A) Stereoview of the least-squares superposition of the crystalline structures of wild-type ribonuclease A (PDB entry 7RSA; blue) and T45G ribonuclease A (red). (B) Stereoview of the electron density ($2|F_o| - |F_c|$) contoured at 1.0 σ of residues surrounding Gly45. Ile81 and Asp83 show static disorder and have been modeled in two side-chain conformations. Phe120 has weak density for its $C_{\epsilon 1}$, $C_{\epsilon 1}$, and C_ζ atoms, indicating some mobility. A water molecule (W1) occupies the position of the side chain of Phe120 from the wild-type enzyme. A chloride ion is also present.

The affinity of RNase A and the T45G variant for tetranucleotides 6-FAM~d(AUAA) and 6-FAM~d(AU^{F}AA) was also determined by fluorescence anisotropy. These values are listed in Table 2. Wild-type RNase A has more affinity for 6-FAM~d(AUAA) than 6-FAM~d(AU^{F}AA). In contrast, T45G RNase A has an approximately equal affinity for 6-FAM~d(AUAA) and 6-FAM~d(AU^{F}AA).

Catalytic Specificity of Ribonuclease A. The values of the kinetic parameter k_{cat}/K_m for the cleavage of four tetranucleotide substrates by wild-type RNase A and the T45G variant were determined in a continuous manner by following the increase of fluorescence after enzyme addition (Figure 5A). These values are listed in Table 3 and depicted in Figure 5B. The values of k_{cat}/K_m for the cleavage of 6-FAM~dArUdAdA~6-TAMRA and 6-FAM~dArCdAdA~6-TAMRA by wild-type RNase A (*15*) are much greater than that for the cleavage of 6-FAM~dArAdAdA~6-TAMRA. The cleavage of 6-FAM~dArGdAdA~6-TAMRA by wild-type RNase A is extremely slow; we estimate the value of k_{cat}/K_m to be <0.1 M^{-1} s^{-1}.

The values of k_{cat}/K_m for the cleavage of 6-FAM~dArUdAdA~6-TAMRA, 6-FAM~dArCdAdA~6-TAMRA, and 6-FAM~dArAdAdA~6-TAMRA by T45G RNase A are more similar than those for cleavage by the wild-type enzyme. As with wild-type RNase A, the cleavage of 6-FAM~dArGdAdA~6-TAMRA by the T45G variant is extremely slow; we estimate the value of k_{cat}/K_m to be <0.5 M^{-1} s^{-1}.

DISCUSSION

Structure of Crystalline T45G Ribonuclease A. The structure of crystalline T45G RNase A was determined at a resolution of 1.8 Å. In this structure, we find no indication of enhanced complementarity of the enzymic active site with an adenine base beyond the mere creation of space. We therefore conclude that the increased ability of T45G RNase

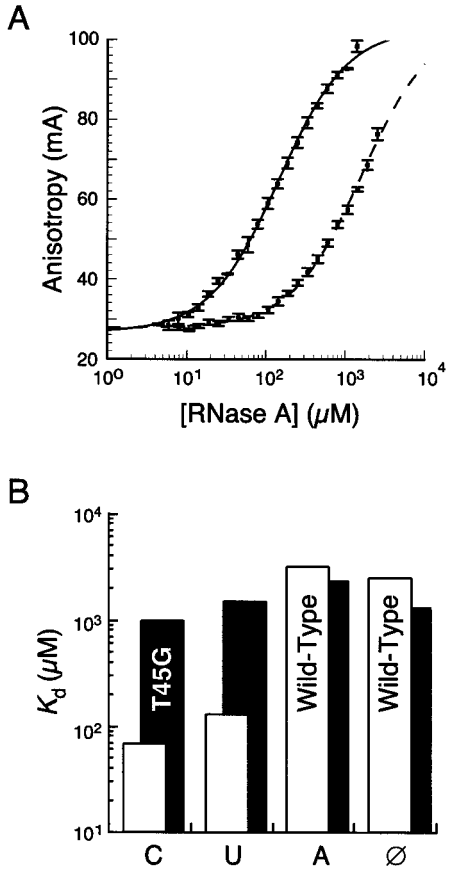

FIGURE 4: Equilibrium dissociation constants. (A) Binding of 6-FAM∼d(UAA) to wild-type ribonuclease A (solid line) and T45G ribonuclease A (dashed line). Binding isotherms were determined with fluorescence anisotropy at (23 ± 2) °C in 0.10 M MES−NaOH buffer (pH 6.0) containing NaCl (0.10 M). (B) Bar graph of the values of K_d for the complexes of wild-type ribonuclease A and T45G ribonuclease A with 6-FAM∼d(XAA), where X is uridine, cytidine, adenine, or an abasic residue (Ø) as depicted in Figure 2.

Table 2. Values of K_d for the Complexes of Wild-Type Ribonuclease A and the T45G Variant with 6-FAM∼d(XAA)[a]

X	wild-type RNase A (mM)	T45G RNase A (mM)
AU	0.012 ± 0.003	0.12 ± 0.02
AU^{F} [b]	0.62 ± 0.22	0.087 ± 0.047
C	0.070 ± 0.002	0.97 ± 0.05
U	0.13 ± 0.01	1.5 ± 0.1
A	3.2 ± 0.1	2.3 ± 0.1
Ø[c]	2.5 ± 0.2	1.3 ± 0.1

[a] Values of K_d were determined by fluorescence anisotropy at 23 ± 2 °C in 20 mM MES−NaOH buffer (pH 6.0) containing NaCl (0.050 M for X = AU, AU^{F}; 0.10 M for X = C, U, A, Ø). [b] dU^{F} refers to 2′-deoxy-2′-fluorouridine. [c] dØ refers to an abasic analogue of DNA (Figure 2).

A to cleave on the 3′ side of adenosine nucleotides arises largely from an expanded B1 subsite. Moreover, we conclude that Thr45 provides specificity not only through hydrogen bonds with pyrimidine bases but also through steric exclusion of purine bases.

In the structure of T45G RNase A, the absence of van der Waals contact with Gly45 results in some disorder and rotation of the side chain of Phe120. This lack of side-chain rigidity is accompanied by movement in the main chain of Phe120. This movement could have an adverse effect on

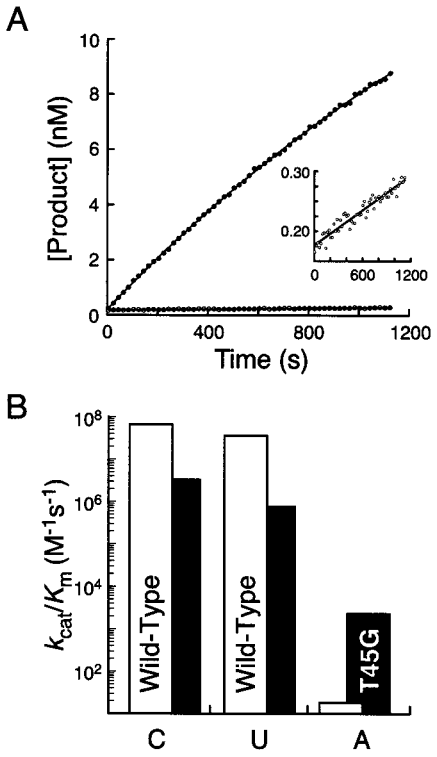

FIGURE 5: Steady-state kinetic parameters. (A) Time dependence of product formation from the cleavage of 6-FAM∼dArAdAdA∼6-TAMRA by wild-type ribonuclease A and T45G ribonuclease A. Values were calculated from the fluorescence emission at 515 nm with excitation at 490 nm upon addition of wild-type RNase A (0.23 μM; ○) or the T45G variant (0.16 μM; ●) using the initial and final fluorescence intensity data of substrate (23 nM). Data for the wild-type and variant enzymes were fitted to eqs 3 and 2, respectively. Reactions were performed at 25 °C in 0.10 M MES−NaOH buffer (pH 6.0) containing NaCl (0.10 M). Inset: Data from the wild-type enzyme plotted with an expanded ordinate. (B) Bar graph of values of k_{cat}/K_m for the cleavage of 6-FAM∼dArXdAdA∼6-TAMRA, where X is uridine, cytidine, or adenine by wild-type ribonuclease A and T45G ribonuclease A.

Table 3. Values of k_{cat}/K_m for the Cleavage of 6-FAM∼dArXdAdA∼6-TAMRA by Wild-Type Ribonuclease A and the T45G Variant[a]

X	wild-type RNase A (10^6 M^{-1} s^{-1})	T45G RNase A (10^6 M^{-1} s^{-1})
C	66 ± 4[b]	3.3 ± 0.3
U	25 ± 3[b]	0.75 ± 0.08
A	0.000018 ± 0.000002	0.0023 ± 0.0002
G	<0.0000001	<0.0000005

[a] Values of k_{cat}/K_m were determined at 25 °C in 0.10 M MES−NaOH buffer (pH 6.0) containing NaCl (0.10 M). Values are the mean (±SE) of triplicate determinations. [b] From ref *15*.

catalysis because the main-chain nitrogen of Phe120 appears to donate a hydrogen bond to the transition state (*10*, *29*).

Nucleobase Binding. We measured the affinity of the wild-type and T45G enzymes for four synthetic DNA ligands. Wild-type RNase A binds 6-FAM∼d(CAA) and 6-FAM∼d(UAA) 20-fold tighter than 6-FAM∼d(AAA) and 6-FAM∼d(ØAA) (Figure 4B). This specificity is all but eliminated by replacing Thr45 with a glycine residue. Interestingly, the loss in specificity is not due to an increase in affinity for adenosine nucleotides but to the loss in binding affinity for cytidine and uridine nucleotides. Despite having the same affinity for adenosine nucleotides as the wild-type enzyme,

T45G RNase A has a much greater capacity to cleave on the 3′ side of adenosine nucleotides (vide infra).

Pentofuranosyl Ring Conformation. Does RNase A interact with RNA and DNA in the same manner? In the crystalline RNase A·d(ATAAG) complex, the active-site base His12 forms a hydrogen bond with a phosphoryl oxygen and is more than 4 Å away from the 2′-carbon of the thymidine (*22*). If the actual Michaelis complex is like the RNase A·d(ATAAG) complex, significant movement would be necessary for His12 to effect catalysis by abstracting a proton from the 2′-hydroxyl group.

The pentofuranosyl ring in a ribonucleoside or 2′-deoxynucleoside can adopt two conformations: N ($C_{3'}$-*endo*-$C_{2'}$-*exo*) or S ($C_{2'}$-*endo*-$C_{3'}$-*exo*). Various steric and stereoelectronic effects of the pentofuranosyl ring (gauche effects) and the nucleobase (anomeric effect) dictate the preference. The prevalence of the N conformation does, however, increase with the electronegativity of the 2′ substituent (*30*). For example, a 2′-fluoro substitution in a 2′-deoxynucleoside makes the pentofuranosyl ring conformation like that in a ribonucleoside (*30*−*34*). Indeed, the 2′-fluorine rather than the phosphoryl group is in contact with His12 in the crystalline RNase S·dU^{F}pA complex (*35*).[3]

We measured the affinity of the wild-type and T45G enzymes for 6-FAM∼d(AUAA) and 6-FAM∼d(AU^{F}AA). Wild-type RNase A binds 6-FAM∼d(AUAA) 50-fold more tightly than 6-FAM∼d(AU^{F}AA). This discrimination, which is surprisingly large, is lost in the T45G enzyme. These data are consistent with a difference in pentofuranosyl ring conformation. In the RNase A·6-FAM∼d(AUAA) complex, a hydrogen bond can likely form between His12 and the 3′-phosphoryl group of the deoxyuridine residue (*22*). A different pentofuranosyl ring conformation in the RNase A·6-FAM∼d(AU^{F}AA) complex could make available only the weaker interaction between His12 and the 2′-fluorine (*35*).[3] In comparison to the wild-type enzyme, T45G RNase A has a low affinity for a uracil nucleobase (Figure 4B). This low affinity may enable a phosphoryl group bound in the active site of the T45G enzyme to interact with His12 regardless of the pentofuranosyl ring conformation.

The interaction of Thr45 with the nucleobase of a pyrimidine nucleoside is less strong when the nucleoside is dU^F, which resembles rU, than dU. This finding suggests that the free energy of the Michaelis complex with RNA is high. Indeed, the pentofuranosyl ring of dG^F is distorted from the N conformation upon binding of dG^{F}pC to ribonuclease Ms (*39*). Such ground-state destabilization mediated by Thr45 could enhance catalysis. Previously, we had shown that Gln11, which like Thr45 is an active-site residue that does not participate directly in the cleavage or formation of covalent bonds, likewise aids catalysis by ground-state destabilization (*40*).

Catalytic Turnover of Cytidine versus Uridine Nucleotides. We measured the ability of wild-type and the T45G enzyme to catalyze the cleavage of four synthetic nucleotide substrates. Wild-type RNase A catalyzes the degradation of 6-FAM∼dArCdAdA∼6-TAMRA slightly more proficiently than 6-FAM∼dArUdAdA∼6-TAMRA, with $(k_{cat}/K_m)_{rU}/(k_{cat}/K_m)_{rC} = 0.55$ (Figure 5B). This substrate specificity is similar to that observed with cytidylyl(3′→5′)adenosine (CpA) and uridylyl(3′→5′)adenosine (UpA) [$(k_{cat}/K_m)_{UpA}/(k_{cat}/K_m)_{CpA} = 0.46$ (*41*) and 0.21 (*42*)], and with cytidine 2′,3′-cyclic phosphate (C>p) and uridine 2′,3′-cyclic phosphate (U>p) [$(k_{cat}/K_m)_{U>p}/(k_{cat}/K_m)_{C>p} = 0.23$ (*13*)].

Like the wild-type enzyme, T45G RNase A cleaves 6-FAM∼dArCdAdA∼6-TAMRA more readily than 6-FAM∼dArUdAdA∼6-TAMRA, with $(k_{cat}/K_m)_{rU}/(k_{cat}/K_m)_{rC} = 0.23$ (Figure 5B). This substrate specificity differs substantially from $(k_{cat}/K_m)_{U>p}/(k_{cat}/K_m)_{C>p} = 0.0096$ (*13*). The ability of the T45G enzyme to distinguish between C>p and U>p is likely to be accentuated by the great reliance of these small substrates on interactions with the enzymic B1 subsite.

Catalytic Turnover of Pyrimidine versus Purine Nucleotides. Wild-type RNase A discriminates greatly against adenosine and guanosine nucleotides. The substrate 6-FAM∼dArAdAdA∼6-TAMRA has only one labile residue, its adenosine *ribo*nucleotide. Wild-type RNase A cleaves on the 3′ side of this nucleotide much more slowly than after the analogous cytidine or uridine nucleotides, with $(k_{cat}/K_m)_{rA}/(k_{cat}/K_m)_{rC} = 3.6 \times 10^{-6}$ and $(k_{cat}/K_m)_{rA}/(k_{cat}/K_m)_{rU} = 2.0 \times 10^{-6}$ (Figure 5B).

T45G RNase A discriminates less against adenosine nucleotides relative to cytidine or uridine nucleotides, with $(k_{cat}/K_m)_{rA}/(k_{cat}/K_m)_{rC} = 7.0 \times 10^{-4}$ and $(k_{cat}/K_m)_{rA}/(k_{cat}/K_m)_{rU} = 3.1 \times 10^{-3}$ (Figure 5B). The rate of cleavage of 6-FAM∼dArGdAdA∼6-TAMRA by both wild-type RNase A and the T45G variant is extremely low ($<0.5\ M^{-1}\ s^{-1}$). Although we cannot quantitate the level of catalytic discrimination of these enzymes against guanosine nucleotides, we can estimate it to be $>10^7$ relative to cytidine or uridine nucleotides.

The ability of T45G RNase A to cleave readily the phosphodiester bond on the 3′ side of adenosine nucleotides was first observed with poly(A) as substrate (*12, 43*). T45G RNase A cleaves poly(A) 1.1×10^2-fold faster than 6-FAM∼dArAdAdA∼6-TAMRA. This comparison is not rigorously correct because the cleavage of poly(A) is processive (*12, 43*), and processive catalysis does not satisfy the approximations used to derive the Michaelis−Menten equation (*44*). The increase in apparent second-order rate constant for poly(A) cleavage is likely to result from the ability of the enzyme to limit the diffusional search for cleavable phosphodiester bonds through processive catalysis. The smaller, 16-fold preference for a polymeric substrate by the wild-type enzyme could reflect the distributive kinetic mechanism of wild-type RNase A.

The efficiency of ribonucleolytic cleavage on the 3′ side of adenosine nucleotides may depend on the conformation adopted by the adenine base. In the most stable conformation of an adenosine nucleoside, the adenine nucleobase adopts an anti conformation about the glycosidic bond. Still, the base can rotate about the glycosidic bond into a syn conformation (*45*). In the syn conformation, the smaller aspect of the adenine base does fit into the B1 subsite of wild-type RNase A, as seen in the structure of the crystalline RNase A·d(AAAA) complex (*46*−*48*). The instability of the syn conformation could contribute to the low rate of 6-FAM∼dArAdAdA∼6-TAMRA cleavage by the wild-type enzyme. Likewise, the greatly enhanced ability of T45G RNase A to cleave after adenosine nucleotides could arise

[3] If the contact between the imidazolium side chain of His12 and the 2′-fluorine of dU^{F}pA is indeed a hydrogen bond, as has been asserted (*35*), then this hydrogen bond is weak (*36*−*38*).

from the ability of the variant to accommodate an adenine base in an anti conformation within its enlarged B1 subsite.

Conclusions. RNase A has prodigious catalytic specificity. This specificity relies on hydrogen bonds between pyrimidine nucleobases and Thr45 as well as the steric exclusion of the anti conformation of an adenine nucleobase by Thr45. A ribose-like ring disfavors the interaction of Thr45 with a pyrimidine nucleobase, suggesting that Thr45 could enhance catalysis by ground-state destabilization. Thus, Thr45 plays an important role in both the nucleobase specificity and substrate turnover of RNase A.

ACKNOWLEDGMENT

We are grateful to Dr. S. B. delCardayré for initiating the study of Thr45 of RNase A and to Prof. I. Rayment, Prof. H. M. Holden, and the members of their research groups for many helpful conversations and for the use of their X-ray data collection and computational facilities, which are supported by Grant BIR-9317398 (NSF).

REFERENCES

1. D'Alessio, G., and Riordan, J. F. (1997) *Ribonucleases: Structures and Functions*, Academic Press, New York.
2. Raines, R. T. (1998) *Chem. Rev. 98*, 1045−1066.
3. Loring, H. S., Carpenter, F. H., and Roll, P. M. (1947) *J. Biol. Chem. 169*, 601−608.
4. Schmidt, G., Cubiles, R., Swartz, B. H., and Thannhauser, S. J. (1947) *J. Biol. Chem. 170*, 759−760.
5. Brown, D. M., and Todd, A. R. (1952) *J. Chem. Soc.* 52−58.
6. Gassen, H. G., and Witzel, H. (1967) *Eur. J. Biochem. 1*, 36−45.
7. Kartha, G., Bello, J., and Harker, D. (1967) *Nature 213*, 862−865.
8. Richards, F. M., Wyckoff, H. W., and Allewel, N. (1970) in *Neurosciences: Second Programme* (Schitt, T. O., Ed.) pp 901−912, Rockefeller Press, New York.
9. Beintema, J. J., Schüller, C., Irie, M., and Carsana, A. (1988) *Prog. Biophys. Mol. Biol. 51*, 165−192.
10. Wlodawer, A., Miller, M., and Sjölin, L. (1983) *Proc. Natl. Acad. Sci. U.S.A.* 80, 3628−3631.
11. Zegers, I., Maes, D., Dao-Thi, M., Poortmans, F., Palmer, R., and Wyns, L. (1994) *Protein Sci. 3*, 2322−2339.
12. delCardayré, S. B., and Raines, R. T. (1994) *Biochemistry 33*, 6031−6037.
13. delCardayré, S. B., and Raines, R. T. (1995) *J. Mol. Biol. 252*, 328−336.
14. Curran, T. P., Shapiro, R., and Riordan, J. F. (1993) *Biochemistry 32*, 2307−2313.
15. Kelemen, B. R., Klink, T. A., Behlke, M. A., Eubanks, S. R., Leland, P. A., and Raines, R. T. (1999) *Nucleic Acids Res. 27*, 3696−3701.
16. Kelemen, B. R., and Raines, R. T. (1999) *Biochemistry 38*, 5302−5307.
17. Kabsch, W. (1988) *J. Appl. Crystallogr. 21*, 67−71.
18. Kabsch, W. (1988) *J. Appl. Crystallogr. 21*, 916−924.
19. Collaborative Computational Project, Number 4 (1994) *Acta Crystallogr. D50*, 760−763.
20. Tronrud, D. E., Ten-Eyck, L. F., and Matthews, B. W. (1987) *Acta Crystallogr. A43*, 489−501.
21. Cambillau, C., Roussel, A., Inisan, A. G., and Knoops-Mouthay, E. (1997) *TURBO−FRODO*, Version OpenGL.1, CNRS/Universite Aix-Marseille II, Marseille, France.
22. Fontecilla-Camps, J. C., de Llorens, R., le Du, M. H., and Cuchillo, C. M. (1994) *J. Biol. Chem. 269*, 21526−21531.
23. Nogués, M. V., Vilanova, M., and Cuchillo, C. M. (1995) *Biochim. Biophys. Acta 1253*, 16−24.
24. Hill, J. J., and Royer, C. A. (1997) *Methods Enzymol. 278*, 390−416.
25. Kelemen, B. R., and Raines, R. T. (1997) in *Techniques in Protein Chemistry VIII* (Marshak, D. R., Ed.) pp 565−572, Academic Press, New York.
26. Fisher, B. M., Ha, J.-H., and Raines, R. T. (1998) *Biochemistry 37*, 12121−12132.
27. Wallace, R. B., and Miyada, C. G. (1987) *Methods Enzymol. 152*, 432−442.
28. Federov, A. A., Joseph-McCarthy, D., Federov, E., Sirakova, D., Graf, I., and Almo, S. C. (1996) *Biochemistry 35*, 15962−15979.
29. Ladner, J. E., Wladkowski, B. D., Svensson, L. A., Sjölin, L., and Gilliland, G. L. (1997) *Acta Crystallogr. D53*, 290−301.
30. Guschlbauer, W., and Jankowski, K. (1980) *Nucleic Acid Res. 8*, 1421−1433.
31. Karpeisky, M. Ya., and Yakovlev, G. I. (1981) *Sov. Sci. Rev., Sect. D 2*, 145−257.
32. Ikehara, M. (1984) *Heterocycles 21*, 75−90.
33. Kawasaki, A. M., Casper, M. D., Freier, S. M., Lesnik, E. A., Zounes, M. C., Cummins, L. L., Gonzales, C., and Cook, P. D. (1993) *J. Med. Chem. 36*, 831−841.
34. Marquez, V. E., Lim, B. B., Barchi, J. J., Jr., and Nicklaus, M. C. (1993) in *Nucleosides and Nucleotides as Antitumor and Antiviral Agents* (Chu, C. K., and Baker, D. C., Eds.) pp 265−284, Plenum Press, New York.
35. Pavlovsky, A. G., Borisova, S. N., Borisov, V. V., Antonov, I. V., and Karpeisky, M. Y. (1978) *FEBS Lett. 92*, 258−262.
36. Shimoni, L., and Glusker, J. P. (1994) *Struct. Chem. 5*, 383−397.
37. Howard, J. A. K., Hoy, V. J., O'Hagan, D., and Smith, G. T. (1996) *Tetrahedron 52*, 12613−12622.
38. Dunitz, J. D., and Taylor, R. (1997) *Chem. Eur. J. 3*, 89−98.
39. Nonaka, T., Nakamura, K. T., Uesugi, S., Ikehara, M., Irie, M., and Mitsui, Y. (1993) *Biochemistry 32*, 11825−11837.
40. delCardayré, S. B., Ribó, M., Yokel, E. M., Quirk, D. J., Rutter, W. J., and Raines, R. T. (1995) *Protein Eng. 8*, 261−273.
41. Witzel, H., and Barnard, E. A. (1962) *Biochem. Biophys. Res. Commun. 7*, 295−299.
42. Follmann, H., Weiker, H. J., and Witzel, H. (1967) *Eur. J. Biochem. 1*, 243−250.
43. delCardayré, S. B., Thompson, J. E., and Raines, R. T. (1994) in *Techniques in Protein Chemistry V* (Crabb, J. W., Ed.) pp 313−320, Academic Press, New York.
44. Chou, K.-C., Kézdy, F. J., and Reusser, F. (1994) *Anal. Biochem. 221*, 217−230.
45. Yathindra, N., and Sundaralingham, M. (1973) *Biopolymers 12*, 297−314.
46. McPherson, A., Brayer, G., Cascio, D., and Williams, R. (1986) *Science 232*, 765−768.
47. McPherson, A., Brayer, G., and Morrison, R. (1986) *Biophys. J. 49*, 209−219.
48. Ko, T.-P., Williams, R., and McPherson, A. (1996) *Acta Crystallogr. D52*, 160−164.
49. Fisher, B. M., Grilley, J. E., and Raines, R. T. (1998) *J. Biol. Chem. 273*, 34134−34138.

BI001862F